Dose-guided patient positioning in proton radiotherapy using multicriteria-optimization

Kurz, C.; Süss, P.; Arnsmeyer, C.; Haehnle, J.; Teichert, K.; Landry, G.; Hofmaier, J.; Exner, F.; Hille, L.; Kamp, F.; Thieke, C.; Ganswindt, U.; Valentini, C.; Hölscher, T.; Troost, E.; Krause, M.; Belka, C.; Küfer, K.; Parodi, K.; Richter, C.;

Originally published:

August 2019

Zeitschrift für Medizinische Physik 29(2019)3, 216-228

DOI: https://doi.org/10.1016/j.zemedi.2018.10.003

Perma-Link to Publication Repository of HZDR:

https://www.hzdr.de/publications/Publ-27339

Dose-guided patient positioning in proton radiotherapy using multicriteria-optimization

Christopher Kurz[a,b], Philipp Süss[c], Carolin Arnsmeyer[d], Jonas Haehnle[c], Katrin Teichert[c], Guillaume Landry[b], Jan Hofmaier[a], Florian Exner[d], Lucas Hille[b], Florian Kamp[a], Christian Thieke[a], Ute Ganswindt[a], Chiara Valentini[e], Tobias Hölscher[e], Esther Troost[d,e,f,g,h], Mechthild Krause[d,e,f,g,h], Claus Belka[a,f], Karl-Heinz Küfer[c]*, Katia Parodi[b]* and Christian Richter[d,e,f,g]*

*authors share senior authorship

[a] *Department of Radiation Oncology, University Hospital, LMU Munich, Marchioninistraße 15, 81377 München, Germanys*

[b] *Department of Medical Physics, Faculty of Physics, Ludwig-Maximilians-Universität München, Am Coulombwall 1, 85748 Garching bei München, Germany*

[c] *Fraunhofer Institute for Industrial Mathematics (ITWM), Fraunhofer-Platz 1, 67663 Kaiserslautern, Germany*

[d] *OncoRay–National Center for Radiation Research in Oncology, Faculty of Medicine and University Hospital Carl Gustav Carus, Technische Universität Dresden, Helmholtz-Zentrum Dresden - Rossendorf, Fetscherstr. 74, PF 41, 01307 Dresden, Germany*

[e] *Department of Radiotherapy and Radiation Oncology, Faculty of Medicine and University Hospital Carl Gustav Carus, Technische Universität Dresden, Fetscherstr. 74, 01307 Dresden, Germany*

[f] *German Cancer Consortium (DKTK), German Cancer Research Center (DKFZ), Im Neuenheimer Feld 280, 69120 Heidelberg, Germany*

[g] *Helmholtz-Zentrum Dresden - Rossendorf, Institute of Radiooncology - OncoRay, Bautzner Landstr. 400, 01328 Dresden, Germany*

[h] *National Center for Tumor Diseases (NCT), partner site Dresden, Germany*

Short title: MCO-based dose-guided positioning in proton therapy

Corresponding author: Dr. Christopher Kurz

Address: Klinik und Poliklinik für Strahlentherapie und Radioonkologie
Klinikum Großhadern
Marchioninistraße 15
81377 München
Germany

Email: christopher.kurz@physik.uni-muenchen.de

Email addresses of all authors: christian.richter@oncoray.de, philipp.suess@itwm.fraunhofer.de, jonas.haehnle@itwm.fraunhofer.de, katrin.teichert@itwm.fraunhofer.de, G.Landry@physik.uni-muenchen.de, jan.hofmaier@med.uni-muenchen.de, Florian.Exner@oncoray.de, Lucas.Hille@physik.uni-muenchen.de, carolin.arnsmeyer@mailbox.tu-dresden.de, florian.kamp@med.uni-muenchen.de, christian.thieke@med.uni-muenchen.de, ute.ganswindt@med.uni-muenchen.de, claus.belka@med.uni-muenchen.de, Katia.Parodi@physik.uni-muenchen.de, christopher.kurz@physik.uni-muenchen.de karl-heinz.kuefer@itwm.fraunhofer.de, Chiara.Valentini@uniklinikum-dresden.de, Tobias.Hoelscher@uniklinikum-dresden.de, Esther.Troost@uniklinikum-dresden.de, Mechthild.Krause@uniklinikum-dresden.de

Submitted to: Zeitschrift für Medizinische Physik

Abstract (300 words)

Proton radiotherapy (PT) requires accurate target alignment before each treatment fraction, ideally utilizing 3D in-room X-ray computed tomography (CT) imaging. Typically, the optimal patient position is determined on the basis of anatomical landmarks or implanted markers. In the presence of non-rigid anatomical changes, however, the planning scenario cannot be exactly reproduced and positioning should rather aim at finding the optimal position in terms of the actually applied dose.

In this work, dose-guided patient alignment, implemented as multicriterial optimization (MCO) problem, was investigated in the scope of intensity modulated and double scattered proton therapy (IMPT and DSPT) for the first time. A method for automatically determining the optimal patient position with respect to pre-defined clinical goals was implemented. Linear dose interpolation was used to access a continuous space of potential patient shifts. Fourteen head and neck (H&N) and eight prostate cancer patients with up to 5 repeated CTs were included in this study. Dose interpolation accuracy was evaluated and the potential dosimetric advantages of dose-guided over anatomy-based patient alignment investigated by comparison of clinically relevant target and organ-at-risk (OAR) dose-volume histogram (DVH) parameters.

Dose interpolation was found sufficiently accurate with average pass-rates of 90% and 99% for an exemplary H&N and prostate patient, respectively, using a 2% dose-difference criterion. Compared to anatomy-based alignment, the main impact of automated MCO-based dose-guided positioning was a reduced dose to the serial OARs (spinal cord and brain stem) for the H&N cohort. For the prostate cohort, under-dosage of the target structures could also be efficiently diminished. Limitations of dose-guided positioning were mainly found in reducing target over-dosage due to weight loss for H&N patients, which might require adaptation of the treatment plan.

Since labor-intense online quality-assurance is not required for dose-guided patient positioning, it might, nevertheless, be considered an interesting alternative to full online re-planning.

Keywords: proton therapy, dose-guided patient positioning, prostate cancer, head and neck cancer

1. Introduction

External beam proton radiotherapy allows for highly conformal dose application to the target volume at reduced integral dose with respect to conventional photon radiotherapy and is thus playing an increasingly important role in the treatment of cancer [1-3]. However, due to the physical properties of protons stopping in matter [4], proton therapy is generally more sensitive to patient positioning inaccuracies and to inter-fractional changes of the patient anatomy [5, 6]. Both sources of uncertainty may result in a decrease of target coverage or an increase of the dose to organs-at-risk (OAR).

Before each treatment fraction, the patient is positioned with the aim of aligning the patient and internal target volume to the iso-center of the beam application system using image-guidance [7]. At most particle therapy facilities, image-guidance still only comprises orthogonal 2D X-ray imaging, but recently also volumetric imaging using either in-room X-ray computed tomography (CT) or cone-beam CT (CBCT) imaging devices has been clinically implemented [8, 9]. Accurate patient alignment is achieved by registration of the in-room control image and the initial planning CT (pCT) that was used for treatment planning. Due to the limited soft-tissue contrast in CT imaging, the target location is often inferred from nearby bony anatomy or implanted radio-opaque markers [10, 11]. Treatment tables allow for a registration with 6 degrees of freedom (d.o.f.), i.e., translation and rotation around three axes [12]. For treatment sessions with no anatomical changes between pCT and daily pre-treatment control CT, the planned dose distribution can be exactly reproduced by accurate rigid alignment (patient positioning). However, in the presence of non-rigid inter-fractional or inter-scan anatomical changes this is not the case. The planning scenario cannot be restored by a 6 d.o.f. rigid transformation and target coverage may be decreased, as well as dose to OARs increased. Thus, it is deemed beneficial to not only focus on implanted markers or anatomical landmarks in the target region for patient alignment in such a scenario, but rather consider directly the dose that would actually be applied to the target structures and OARs at a given position of the patient with respect to the beam application system.

Another use-case of dose-based patient positioning are complex anatomies with many degrees of freedom (e.g., knee joints or the head and neck (H&N) region), where it can be very time-consuming to exactly reproduce the patient position of the pCT needing many iterations. Also here it would be beneficial to find a position that optimally recovers the dosimetric properties of the plan independent from slight anatomical differences.

Two specific treatment sites that might benefit from such a dose-guided patient positioning in proton therapy are H&N and prostate [13-15]. For H&N cancer patients, typical non-rigid inter-fractional changes are weight-loss and alterations in the neck tilt [16-18]. For prostate cancer patients, variability of rectum and bladder filling, also affecting the position of the prostate itself [19-21], or rotations of the femoral heads, can considerably alter and compromise the applied treatment [22, 23]. Bladder and rectum filling variations can be minimized by the use of sophisticated positioning protocols including the application of water-filled rectum balloons and drinking protocols, however, slight variations can always occur especially if the compliance with the drinking protocol is not optimal or when there are delays in the treatment delivery.

When considering directly the applied dose for determining the optimal patient position in these scenarios, dose to the target structures and to the relevant OARs has to be taken into account and traded off against each other. Consequently, dose-guided positioning has to be considered as a multi-criterial optimization (MCO) problem with a whole set of Pareto-optimal solutions [24], i.e., patient positions or shifts.

Dose-guided positioning in the context of proton therapy has initially been suggested by Cheung et al. [25]. In their study, a variety of discrete patient shifts was evaluated in terms of their corresponding dose distribution and correlated dose-volume-histogram (DVH) parameters in order to select the most favorable patient position. Although the impact on target as well as OAR dose was considered, the dose-guided positioning was not strictly treated as MCO problem. In the scope of conventional photon radiotherapy, however, the implementation of dose-guided patient

positioning as MCO problem, based on user-defined clinical goal functions for target structures and OARs, has been recently presented by Haehnle et al. [26]. The described implementation particularly allows the user to interactively browse and navigate through the set of Pareto optimal patient shifts in order to find the position which yields the clinically preferred dose distribution on basis of the daily patient anatomy. By using linear dose interpolation, a continuous range of patient shifts can be accessed, while the specific implementation assures Pareto optimality of each patient position with respect to the pre-defined clinical goals during navigation. A first application of this method using daily (CBCT) images was recently described in Hofmaier et al. [27].

In this work, we present the first application of MCO-based dose-guided patient positioning to proton therapy, using the same framework described by Haehnle et al. In addition to the implementation described in that work, a functionality to automatically determine the optimal shift according to the user-defined clinical goals was implemented and used for dose-guided patient alignment for the first time. The methodology was evaluated for the treatment sites of H&N and prostate in the scope of intensity-modulated proton therapy (IMPT) using pencil beam scanning as well as in the scope of single field uniform dose technique (SFUD) using double-scattered proton therapy (DSPT). The main goal of this proof-of-principle study was in particular to identify potential clinical benefits from MCO-based dose-guided patient alignment in the presence of non-rigid anatomical changes with respect to the currently clinically used anatomy- or marker-based alignment procedure.

2. Material and methods

2.1 Patient cohorts and CT data

The available patient data was split into the IMPT and DSPT cohort, respectively.

IMPT patient cohort

Eleven H&N cancer patients (HN1-11), as well as five prostate cancer patients (PRO1-5) have been considered in this work. All patients were originally treated with intensity-modulated radiotherapy (IMRT) at the Department of Radiation Oncology at LMU Munich (Germany).

For each of these patients, a planning CT (pCT) was acquired with a Toshiba Aquilion LB CT scanner (Toshiba Medical Systems, the Netherlands) at a voxel size of 1.074 x 1.074 x 3.0 mm. For patients HN1-11, a replanning CT (rpCT) acquired 25 to 51 days after the initial pCT during the course of fractionated treatment with the same scanner and settings was considered as surrogate for volumetric daily pre-treatment imaging and used for dose-guided positioning. For patients PRO1-5, three repeated CTs have been acquired on consecutive days for monitoring the inter-fractional motion. No bladder or rectum filling protocol was applied. In our study, the first CT was considered as pCT, the repeated second and third CT (also referred to as rpCT) as surrogate for the daily control image during dose-guided alignment.

DSPT patient cohort

For this cohort, three H&N cancer patients (HN12-14), as well as three prostate cancer patients (PRO6-8) have been considered. All of them were originally treated with double-scattered proton therapy (DSPT) at the proton therapy facility of the Carl Gustav Carus University Hospital Dresden (Dresden, Germany) between March and September 2015. All patients expressed written informed consent.

For each of these patients, a planning CT (pCT) was acquired with a Somatom Definition AS single-source CT scanner (Siemens Healthineers, Forchheim, Germany). A sequential dual energy CT (DECT) scan (80/140 kVp) with 0.977 x 0.977 x 2.0 mm voxel spacing was used. The clinical proton treatment is planned on a 79 keV pseudo-monoenergetic CT [28]. For each patient, five repeated controls CT (referred to as rpCT in this study) scans acquired with an in-room CT (same type as planning CT, same acquisition and reconstruction procedure) during the course of treatment (between fraction 2 and 34, 11 to 32 control CTs available per patient) were selected,

except for HN14 with only four control CTs available during the analyzed treatment series. There was at least a one week time duration between the evaluated control CTs.

For the prostate treatments, an in-house positioning protocol was applied, including the application of a water-filled rectum balloon and a strict drinking protocol to minimize intra- and inter-fractional prostate movements and to increase positioning reproducibility. H&N patients were immobilized with a thermoplastic head-and-shoulder mask, similar to the IMPT cohort.

General

Note that within this study, the clinical origin of the repeated CTs (either acquired for replanning or as (in-room) control CT) was not of relevance, so the same abbreviation (rpCT) was used in all cases. All pCTs and rpCTs were delineated by trained physicians. Note that the availability of up-to-date contours is a pre-requisite for performing dose-guided positioning. Every rpCT was rigidly registered to the corresponding pCT using a 6 d.o.f. registration in the treatment planning system mimicking the anatomy-based alignment applied before treatment. For the H&N patients, registration aimed at matching the bony anatomy in the central region of the target (first to sixth vertebrae). Similarly, registration aimed at matching the bony anatomy of the pelvic bones in vicinity of the target volume for the prostate patients. This bony anatomy-based registration was later on considered as reference scenario (anatomy-based positioning) and utilized as starting point for dose-guided alignment.

2.2 Treatment planning

IMPT treatment planning

For all IMPT cohort patients, new IMPT treatment plans were generated for this study on the respective pCT using a research version of the commercial treatment planning system (TPS) RayStation (version 4.99, RaySearch, Stockholm, Sweden).

Following the original clinical prescription, all H&N patients, except from HN1, received a simultaneous integrated boost (SIB) treatment with two dose levels prescribed to a low and a high dose planning target volume (PTV). The high dose PTV surrounded the high dose clinical target volume (CTV) around the gross tumor volume (GTV), while the low dose PTV extended the low dose CTV covering the lymphatic pathways. In both cases, a CTV to PTV margin of 7 mm was applied. Low dose PTV prescriptions ranged from 50.0 Gy to 54.4 Gy, high dose PTV prescriptions from 56.0 Gy to 66.0 Gy in 25 to 32 treatment fractions. For all PTVs, a $V_{95\%}$ of 100% was targeted during treatment planning, while maximum dose to the PTV (D_{max}) should not exceed 105% of the prescribed dose (D_{prescr}). For evaluating D_{max} in the low dose PTV, the high dose PTV region, extended by a 5 mm margin, was excluded. In terms of the OARs, planning objectives included a parotid gland mean dose (D_{mean}) below 26 Gy, as well a D_{max} below 45 Gy and 54 Gy to the spinal cord and the brain stem, respectively. For patients HN8-11 with more cranially located target volumes at the sinuses and nasal cavity, planning objectives for the optical system were added: D_{max} below 54 Gy and 56 Gy for the optical nerves and the chiasm, as well as D_{mean} below 10 Gy for the eye lenses. For patients HN1-7 beams from four different gantry angles of 45°, 90°, 270° and 315° on the International Electrotechnical Commission scale were simultaneously optimized, with the beams from 90° and 270° blocked in the shoulder region. For the more cranial lesions (HN8-11) only three gantry angles of 0°, 100° and 260° were used, the 0° beam blocked in the region of the oral and nasal cavities.

For the prostate patients, fully modulated IMPT plans were generated using two opposing beams from 90° and 270° gantry angle. Based on the estimated prostate motion on the repeated CT imaging data, a 10 mm CTV to PTV margin was applied. The prescribed dose to the PTV ranged from 70 Gy to 76 Gy in 2 Gy fractions. The lymphatic pathways were not considered. Treatment planning aimed at PTV $V_{95\%}$ of 100%, with D_{max} in the PTV below 105% of D_{prescr}. For the OARs, following the QUANTEC report [29], planning aimed at rectum V_{50Gy}<50%, V_{60Gy}<35%, V_{65Gy}<25% and V_{70Gy}<20%, as well as bladder V_{65Gy}<50% and V_{70Gy}<35%.

DSPT treatment planning

For all DSPT patients, the clinical DSPT treatment plans, generated with XIO (Elekta AB, Stockholm, Sweden) were used in this study. Range (±3.5%+2 mm) and setup uncertainties (3 mm) were considered in the double-scattered treatment planning by aperture expansion and range selection. In DSPT planning no PTV concept is used, as the uncertainties are included beam-specific and non-isotropic as described above. For all CTVs, a $V_{95\%}$ of 100% was targeted during treatment planning, while maximum dose to the CTV (D_{max}) should not exceed 105% of the prescribed dose (D_{prescr}). For evaluation RayStation (version 4.99) was used, similar to the IMPT cohort.

Two H&N DSPT patients (HN12+13) with unilateral H&N cancer, received a sequential boost treatment with two dose levels prescribed to a low and a high dose CTV, similar to the IMPT planning. 25 and 8 fractions were used for the two treatment series (50+16 Gy), respectively. For HN14 a single high dose CTV was planned (30 fractions, 60 Gy) for a tongue cancer. For the evaluated non-boost series, always two beams were used with beam angles ranging between 270-290° and 325-350°, respectively. In terms of the OARs, planning objectives included a parotid gland mean dose (D_{mean}) below 26 Gy, as well a D_{max} below 45 Gy, 54 Gy and 56 Gy to the spinal cord, the brain stem and brachial plexus, respectively.

Two prostate DSPT patients (PRO7+8), received a sequential boost treatment with two dose levels prescribed to a low and a high dose CTV – 29 and 8 fractions for the two treatment series (58+16Gy), respectively. The high risk CTV contains the prostate with a 4 mm margin, whereas the low-risk CTV contains the high risk volume plus the base of the seminal vesicle with an additional global 4 mm margin. For PRO6 a single high dose CTV was planned (37 fractions, 74 Gy). Two opposing beams from 90° and 270° gantry angle were used in all cases. For the OARs, following the QUANTEC [29] and PREFERE [30] reports, planning aimed at rectum V_{40Gy}<55%, V_{50Gy}<50%, V_{60Gy}<35%, V_{65Gy}<25% and V_{70Gy}<20%, V_{75Gy}<15% with the V_{76Gy}<2cm^3, as well as

bladder V_{65Gy}<50%, V_{70Gy}<35% and V_{75Gy}<25%. Femoral heads should receive a V_{52Gy}<5% and penile bulbs a V_{50Gy}<90% as well as V_{70Gy}<70%.

For all DSPT patients only the first series (low dose CTV) was evaluated for consistency. Dose constraints were scaled from the total treatment to this first series based on the prescribed dose.

2.3 MCO-based dose-guided positioning

A detailed description of the exact implementation of MCO-based dose-guided patient positioning used in this study can be found in Haehnle et al. [26]. In the following, only the main ideas and steps will be outlined.

The optimization problem to be solved in the scope of dose-guided patient alignment is to find the iso-center position, or equivalently the corresponding patient shift, that yields the best possible dose distribution within the patient under consideration of a set of user-defined clinical goal functions describing, e.g., target coverage and dose limits to OARs. If more than one single clinical goal is defined, the iso-center optimization is a multi-criterial problem to which no single best solution exists. Instead, there is a whole set of Pareto optimal solutions.

As a starting point for multi-criterial position optimization, the bony anatomy-based alignment of the daily CT (rpCT) to the pCT is used and the dose of the initial treatment plan recalculated, using the same pencil-beam algorithm that was used during plan optimization. The result is the so-called *central dose*, corresponding to the standard clinical alignment. Starting from this central position, the iso-center is shifted by ±3 mm and ±6 mm along each of the three axes and the dose recalculated for each of these *sample points*. Given the required calculation time, dose can only be evaluated at a limited number of *sample points* (13 in the current implementation) although the space of Pareto optimal solutions is continuous. In order to allow for a continuous space of potential patient shifts, the dose is linearly interpolated between the pre-calculated *sample points*,

such that all patient positions within their convex hull become accessible. However, for the sake of improved accuracy, interpolations using two sample points at ±6 mm shift were excluded [26].

In order to find the clinically most suitable iso-center shift, the user can define a variety of different clinical goal functions, e.g., describing deviations from the originally planned dose to the targets or OARs. In this study, only clinical goal functions Q_i were used that quantify directly the deviation of a certain DVH parameter d_i, such as $D_{2\%}$, D_{mean}, $V_{95\%}$ or V_{60Gy}, when comparing the dose of the treatment plan P on the daily image at a given patient shift c [$D_{rpCT}(c,P)$] to the dose of the original plan on the pCT [$D_{pCT}(P)$]:

$$Q_i(P,c) = d_i(D_{rpCT}(c,P)) - d_i(D_{pCT}(P)) \quad (1)$$

A detailed overview of the clinical goals used in this study is given in Table 1. Instead of the deviation of a certain DVH parameter with respect to the initial planning scenario [$D_{pCT}(P)$], also the deviation to a fixed value for the given DVH parameter can be used in a clinical goal function. For OARs, the clinical goal function will only penalize over-dosage, for target structures only under-dosage.

For each clinical goal function, the minimum and maximum value is evaluated considering their values at the 13 pre-calculated *sample points*. Within the implementation of the ITWM research software MIRA (Multicriteria Interactive Radiotherapy Assistant) utilized for this study, so-called *Pareto sliders* are then set up for each individual clinical goal and enable to interactively browse the space of Pareto-optimal solutions. Each slider configuration is transferred to a corresponding Pareto-optimal iso-center shift. The respective dose is interpolated in real-time and displayed to the user, thus allowing him to straightforwardly determine a clinically beneficial dose-guided shift [26, 31].

For the present study, an additional feature has been implemented in MIRA that allows to directly find the optimal patient position/iso-center shift according to the user-defined clinical goals. It automatically proceeds iteratively through the *importance classes* defined by the user (starting

with the lowest value), and tries to fulfill exactly all of the clinical goals belonging to that class. If it is not possible to achieve all goals of the current importance class, the patient shift is determined such that it minimizes the worst violation of any current goal, and the method stops. If, however, such a plan exists, it sets these achieved goals (and all previously achieved goals) as hard constraints and proceeds to the next importance class. As such, it is reminiscent of the *epsilon constraint method* (see [32] and references therein) in the theory of multicriteria optimization. The linear optimization problems posed this way are modifications of the problems solved during Pareto navigation [31] and can be solved in real-time.

2.4 Data evaluation

For every patient included in this study, the optimal shift according to the pre-defined clinical goals (see Table 1) was determined using the previously described algorithm and the anatomy-based alignment of the daily rpCT to the pCT as starting point. For each determined shift, the exact dose distribution was recalculated in RayStation and DVH parameters were extracted for evaluation within this study. The dosimetric consequences of MCO-based dose-guided positioning were evaluated by comparison of clinically relevant DVH parameters as obtained for the central dose (anatomy-based alignment) and for the determined optimal shift (dose-guided alignment). The DVH parameters for anatomy- and dose-guided positioning were also compared with those of the initial treatment plan. For all patients, CTV $D_{98\%}$ and PTV $D_{2\%}$ (IMPT) or CTV $D_{2\%}$ (DSPT) were included for data analysis. In terms of the OARs, the same DVH parameters used as clinical goals during dose-guided positioning were evaluated (see Table 1). Statistically significant differences between the DVH parameters for anatomy-based and dose-guided alignment were determined by means of a paired Wilcoxon signed-rank test at a significance level of $p=0.05$.

For validation of the dose estimation capability of the dose-guided positioning approach in MIRA, the linearly interpolated dose distribution estimated by MIRA for the obtained shift was compared to the exact calculation from RayStation. For further analyzing the interpolation accuracy, interpolated and exact dose calculations were compared for 20 random shifts for one exemplary

H&N (HN3) and one exemplary prostate case (PRO1). Differences in interpolated and exact dose were quantified using a 2% dose difference criterion, considering only voxels receiving at least 20% of the prescribed dose.

For one case (HN4) where the automatic shift according to the defined clinical goals yielded unsatisfactory results, a clinically preferable patient shift was determined manually using the Pareto-navigation implemented in MIRA. This case will be discussed separately.

3. Results

3.1 Determined shifts and interpolation accuracy

An overview of the retrieved shifts according to the pre-defined clinical goals with respect to the central anatomy-based alignment is given in Tables 2 and 3 for all H&N and prostate cases, respectively. For the H&N patients, most shifts appeared in the anterior-posterior (AP) and superior-inferior (SI) direction. Shifts along these axes are most strongly correlated to changes in dose to the target (AP and SI), as well as dose to the spine (AP) and brainstem (AP and SI) which were treated with highest priority in the dose-guided positioning optimization.

Similarly, with a few exceptions, dose-guided shifts for the evaluated prostate patients were mainly in AP and SI direction. The applied opposing-field plan setup is largely invariant to left-right (LR) shifts, whereas AP and SI shifts directly affect dose to the targets and OARs. For 76% of the evaluated prostate patient positioning cases the dose-guided shifts were found coinciding with one of the pre-calculated sample points.

Concerning the evaluation of the accuracy of the interpolated dose distribution in MIRA at the obtained shifts, pass-rates ranging from 76.0% to 99.7% for H&N cases and from 94.7% to 99.5% for prostate cases were found (Tables 2 and 3), excluding the shifts to so-called sample points. Pass-rates were comparable for IMPT and DSP cohorts. The pass-rates determined at 20 random shifts for exemplary patients HN3 and PRO1 are shown as boxplots in Figure 1. For patient HN3,

the mean pass-rate was 90±2% (1σ). For patient PRO1, a higher mean pass-rate of 99.2±0.4% was found. Deviations between interpolated and exact dose calculation were most pronounced at the patient surface (c.f. Figure 1), where the dose increases from 0 Gy to values of up to 50 Gy from one pixel to the next, such that inaccuracies in the interpolation cannot be avoided. For the prostate cases on the other hand, dose at the surface is below 20% of the prescription and thus not considered during evaluation, hence leading to higher dose-difference pass-rates. Since the dosimetric evaluation of the two positioning approaches (anatomy-based and dose-guided) is based exclusively on exact recalculations, it is not affected by any interpolation effects.

3.2 Dosimetric evaluation

3.2.1 H&N

An overview of the dosimetric impact of the determined patient shifts on the considered target and OAR DVH parameters for the H&N patients is given in Figures 2 and 3 for the IMPT cases and in Figure 4 for the DSPT cases, respectively. All values are given for the whole course of fractionated treatment, i.e., number of fractions times fraction dose for each patient.

For the target structures of the IMPT cases, the main impact of the anatomical changes appearing between pCT and rpCT, i.e., weight-loss and variations of the neck tilt, was found to be a decrease of $D_{98\%}$ and $V_{95\%}$ in the low dose PTV, as well as a considerable increase in low and high dose PTV $D_{2\%}$ (Figure 2, left). In terms of the OARs, anatomical changes caused an increased dose to the spinal cord and the eye lenses (Figure 3, left). When applying the dose-guided shifts, dose to the spinal cord, brain stem and eye lenses was reduced. Differences between anatomy-based and dose-guided shift were, however, below 2 Gy for the OARs and statistically not significant (Figure 3, right). The low dose CTV $V_{95\%}$ could be slightly improved by the dose-guided shift, at the expense of an increased low dose PTV $D_{2\%}$. Both these changes were statistically significant, but median changes were below 1.5 Gy (Figure 2, right). For a few cases, the dose-guided shift led to

a clearly increased dose (by about 5 Gy for the whole course of treatment) to some of the OARs with respect to the anatomy-based. In these cases, however, OAR dose was well below tolerance.

For the DSPT cases (Figure 4), in general comparable results were achieved: target coverage was slightly reduced on the rpCTs, probably due to anatomical changes. As sequential boost or single series treatments were evaluated, hot-spots were not a problem (D_2 was practically unchanged). In the course of the treatment, only minor changes to spinal cord and parotid doses were observed. The dose to the brainstem was in general reduced for both positioning approaches. However, there was an exception in the two last evaluated fractions of patient HN12. This was caused by a reduction of tissue in the high-dose target region close to the patient surface visible in the rpCTs, probably caused by weight loss combined with tumor shrinkage. The brainstem was located distal to the treatment field. The anatomical changes caused a relevant increase of the brainstem D_2 value from 11.5 Gy in the pCT to around 30 Gy in the last fraction, still far below the constraint of 54 Gy. Interestingly, in the second-to-last evaluated fraction (HN12-4) dose-guided positioning could compensate the anatomical change by a shift in SI direction recovering the brainstem dose of the pCT, whereas anatomical positioning could not, resulting in a brainstem D_2 increase of about 13 Gy (+47%). However, this superiority in terms of brainstem sparing was not statistical significant, probably due to the low number of data points (5) as the brainstem was spared completely in all other DSPT patients. Similar to the IMPT cohort, differences between the two positioning approaches concerning target coverage were small and not statistical significant.

The only clinically not acceptable automatically determined dose-guided shift was retrieved for patient HN4 from the IMPT cohort, where the dose-guided shift according to clinical goals (0.0 mm, 0.0 mm and 3.0 mm in LR, AP and SI) resulted in a high dose CTV $V_{95\%}$ decrease by more than 13% with respect to the anatomy-based alignment. This is likely attributed to the fact that only CTV $D_{98\%}$, but not CTV $V_{95\%}$ was included in the pre-defined clinical goals of the dose-guided positioning. Nevertheless, for this single case, a clinically satisfying dose-guided shift could be manually determined using the implemented Pareto-sliders of the MIRA positioning tool. The

resulting DVH curves are shown in Figure 5. Using the manual dose-guided shift of -0.81 mm, -1.32 mm and 0.87 mm in LR, AP and SI, the high dose CTV $V_{95\%}$ could be increased from 85.6% to 99.6% at the expense of a 1 Gy increase of the mean dose to the left parotid gland, which was, however, still below the planning scenario. Compared to the anatomy-based shift, the manual dose-guided shift had an about 1% higher $V_{95\%}$ in the high and low dose CTV and a 2 Gy lower spinal cord $D_{2\%}$ for this patient.

3.2.2 Prostate

An overview of the changes in the considered DVH parameters for the IMPT prostate cancer cohort is given in Figures 6 and 7 for the target structures and OARs, respectively. Compared to the planning scenario (left panel of Figures 6 and 7), target coverage was decreased on the rpCTs. Moreover, there were substantial changes in dose to the OARs for most patients due to the pronounced inter-fractional anatomical changes. In particular, there was a trend for increased dose to the bladder at slightly reduced dose to the rectum (Figure 7, left). Comparing anatomy-based and dose-guided positioning (right panel of Figures 6 and 7), dose to the bladder could be slightly reduced, at the expense of a slightly increased V_{50Gy} to the rectum. None of these changes were statistically significant and median differences were below 2.5%. For the target structures, median differences between anatomy- and dose-based alignment were even smaller (below 0.5 Gy/0.5%). Still, a significantly increased CTV $V_{95\%}$ was found after dose-guided positioning. Particularly for two cases with considerably reduced target coverage with respect to the planning scenario (CTV $V_{95\%}$ reduced by 5/10%), dose-guided alignment was able to considerably improve target coverage (CTV $V_{95\%}$ increased by 4/9%), resulting in a clinically favorable dose distribution (Figure 6, right).

For the DSPT cohort, less variation in target coverage and rectum dose was found compared to the pCT (Figure 8, left), indicating the effectiveness of the applied positioning protocol (e.g., water-filled rectum balloon). Similar to the IMPT cohort, variations in the bladder dose parameters were present. Based on our clinical experience, this is mostly caused by remaining variations in bladder

filling although a drinking protocol was applied. All variations were clinically not relevant, also confirmed by a full dose accumulation for the anatomy based positioning [8]. Comparing the two positioning approaches (Figure 8, right), dose-guided positioning yielded a small but significant improvement of target coverage. In 80% of the investigated cases, the D98 was higher compared to anatomy-based positioning. For the OAR, no clear trend was seen (non-significant differences). So except the influences of the different bladder and rectum immobilization protocols, the results concerning the evaluation of dose-guided vs. anatomy-based positioning are similar between the IMPT and DSPT cohort.

4. Discussion

In this study, MCO-based dose-guided patient positioning has been successfully applied for the first time in the scope of proton therapy considering cohorts of H&N and prostate cancer patients. Using linear dose interpolation between pre-calculated control points, a continuous space of Pareto-optimal patient shifts was accessible. A fully automatic algorithm to find the optimal patient position with respect to the pre-defined clinical goals was implemented and successfully applied for the first time.

As a pre-requisite, the accuracy of the utilized linear dose interpolation was investigated for the generated IMPT plans of two exemplary patients and random shifts. Compared to the exact dose calculation, satisfactory mean pass-rates of about 90% for H&N and 99% for prostate were found, using a 2% dose-difference criterion. In previous studies, similar pass-rates were found using IMRT plans [26, 27]. This result is not obvious, as the proton dose distribution is highly non-linear due to the Bragg peak and the resulting dose gradients. Deviations appeared mainly at the patient surface for H&N patients, due to the steep dose increase at the outer patient contour. These kinds of interpolation inaccuracies will, however, mainly affect the determination of DVH parameters describing the coverage of the PTV (e.g., PTV $D_{98\%}$) which can reach up to the patient surface. Such DVH parameters, affected by patient surface effects, have not been included in the clinical

goals defined in this work and should preferably be avoided in the scope of dose-guided positioning in general. For the smaller CTV, e.g., the impact of dose interpolation inaccuracy at the surface is less pronounced, but should be carefully kept in mind during dose-guided positioning. Interpolation accuracy was higher for prostate patients since the surface dose level was below the threshold used for evaluation.

The newly developed algorithm to automatically determine the optimal shift according to the pre-defined clinical goals gave meaningful results in all investigated cases but one (HN4). Thus, a fast, straight-forward and reproducible workflow for online dose-guided position adaptation seems feasible, since no user interaction is required to determine the optimal shift. Nevertheless, in cases where the automatically obtained shift is not satisfying, manual adjustment can easily be accomplished using the implemented navigation in the space of Pareto optimal solutions. Hence, the evaluated approach has the potential to be clinical-routine changing with a benefit especially in complex cases.

When automatically determining the best patient position, it was noticed that shifts often coincided with one of the pre-calculate sample points, particularly for the prostate cohort. This is directly related to how it was chosen to solve the given linear optimization problems: If any goal of the current importance class cannot be achieved, it is likely best approximated by an extreme shift, which coincides with one of the sample points defining the boundary of the region that can be attained by positioning. This behavior could, in the future, be modified by not minimizing the worst violation of all goals of one importance class but, e.g., their average violation.

Our study showed that dose-guided positioning can be an efficient tool for improving target coverage, especially for prostate cancer patients, where CTV $V_{95\%}$ could be increased by up to 14%. Such effects might become even more striking when going to smaller safety margins, accounting for patient set-up uncertainties and potential anatomical changes, and to scenarios without bladder and/or rectum filling protocol: In such a scenario, dose-guided positioning could be

utilized to compensate for dosimetric deviations related to inter-fractional anatomical changes by patient alignment instead of solely by safety margins or robust optimization. Our results also suggest that dose-guided positioning can efficiently be used to prevent over-dosage to serial OARs, such as the brainstem (dose reduced by 47% in HN12) and the spinal cord. In this context, selection of the defined clinical goals is important: Spinal cord and brain stem were attributed to a higher importance class, resulting in a corresponding trend towards smaller $D_{2\%}$ values of these OARs by dose-guided alignment with respect to anatomy-based positioning. Each center can decide individually and treatment-site specifically which of the clinical goals are considered most important and tune the applied clinical goals and importance classes accordingly. As mentioned before, in case of unsatisfactory results, the weighting of the different goals can be manually adapted by an authorized person.

Nevertheless, it should be noted that only few systematic trends could be identified when comparing the daily dose distributions form anatomy- and dose-based patient alignment and that average dosimetric changes were rather small, mostly within 2 Gy or 2% for the considered median DVH parameters. In particular, dose-guided positioning was not able to properly account for increasing PTV $D_{2\%}$ in the IMPT cases, while keeping satisfying CTV coverage for the H&N cohort. This is likely related to the fact that the increase in PTV $D_{2\%}$ is attributed mainly to patient weight-loss and/or tumor shrinkage, which could only be accurately compensated by plan adaptation. In general, the capabilities of dose-guided positioning are deemed more limited in proton therapy compared to photon therapy, due to the higher sensitivity of the dose distribution to anatomical changes and the increased complexity of the treatment featuring a larger number of free parameters (especially the proton energy/range) at the planning stage. In consequence, dosimetric changes due to changing patient anatomy can be more complex and more difficult to correct by dose-guided positioning. Still, in case of anatomical changes affecting the dose distribution in the patient, the approach can be able to mitigate the effect in the first instance (as

for HN12-4 brainstem dose) so that a treatment can still be safe and possible and there is time to generate an adapted plan for the succeeding fractions.

Potentially, results achieved by dose-guided positioning could be further improved by including also patient rotations and not only shifts. Although it would require a considerably increased number of pre-calculated sample points this issue might be tackled in the future.

An alternative to dose-guided patient alignment for restoring the originally planned dose distribution is full online re-planning, using the available daily imaging data and contours, which are both also required for dose-based positioning. While re-planning will enable restoring the original plan quality in most cases, the newly optimized treatment plan requires inspection and acceptance from a trained physician, as well as patient specific quality assurance (QA) prior to treatment. In the scope of proton therapy, plan QA up to date often includes irradiation of the generated plan to a phantom featuring ionization chamber arrays for dose comparison to the TPS, and is a time-consuming and work-intensive procedure. As pointed out in the previous work by Haehnle et al [26], dose-guided patient alignment does not require any form of labor-intense QA procedure, thus eventually allowing for a faster workflow to improve the applied dose of the day. Since the treatment plan itself remains unchanged, dose-guided positioning might in addition not strictly require the presence of a trained physician during each patient treatment. Given the rather short time required for calculating the sample dose distributions and for setting up the dose-guided positioning optimization problem, in combination with the newly implemented automatic shift determination, fast online application of dose-guided patient positioning seems feasible. More details on the exact time required in such a workflow can be found in Haehnle et al. It could be a pragmatic approach as long as online adaptation has not been translated into clinical routine.

It should be noted, that for the IMPT cohort, diagnostic CT imaging data, acquired for (re-)planning purposes in a separate room, were used as surrogate for daily volumetric in-room imaging. In a clinical scenario, this data would have to be replaced by in-situ imaging data acquired, e.g., with a

gantry- or table-mounted CBCT system following intensity correction [33-35] or with a dedicated in-room CT [8] as used for the DSPT cohort.

A bottleneck for dose-guided positioning is the availability of up-to-date contours on the daily imaging data, which are required for evaluation of the pre-defined clinical goals. Preferably, contours should be available fully automatic and within a few seconds. Promising results were obtained using deformable image registration (DIR) warping the contours from the planning CT, e.g., to the daily CBCT [33, 36] or repeated CT. Implemented on graphical processor units, this is a potentially very fast solution [37]. Still, DIR-based contour propagation is challenging and accuracy can be limited, particularly in regions affected by pronounced anatomical changes [38, 39]. More advanced atlas- or deep learning-based approaches promise improved and fast auto-segmentation in the future [40, 41].

5. Conclusions

MCO-based dose-guided patient positioning using an algorithm automatically determining the optimal patient shift according to pre-defined clinical goals was successfully applied in the scope of proton therapy. With respect to anatomy-based alignment, dose-guided positioning enabled enhanced sparing of serial OARs (H&N) and improved target coverage (prostate) in the presence of inter-fractional anatomical changes. Similar results concerning the benefit of dose-guided positioning were found for IMPT and DSPT cohorts, underlining the applicability for both treatment modalities. Limitations were identified in mitigating over-dosed regions in the target volume (for IMPT H&N treatments). Still, dose-guided patient positioning might be considered an interesting, faster and less complex alternative to full online re-planning in proton therapy.

Acknowledgements

This work was supported by the Federal Ministry of Education and Research of Germany (BMBF), Grant No. 01IB13001 (SPARTA) and Grant No. 03Z1N51 (High Precision Radiotherapy Group at OncoRay), and by the German Research Foundation (DFG) Cluster of Excellence Munich-Centre for

Advanced Photonics (MAP). The prompt help of Nils Peters (OncoRay) for the generation of the DSPT boxplots is gratefully acknowledged. We also thank Erik Traneus and RaySearch for their support with the RayStation TPS.

There are no conflicts of interest.

References

[1] Durante M, Loeffler JS. Charged particles in radiation oncology. Nat Rev Clin Oncol 2010;7:37-43.

[2] Loeffler JS, Durante M. Charged particle therapy--optimization, challenges and future directions. Nat Rev Clin Oncol 2013;10:411-24.

[3] Baumann M, Krause M, Overgaard J, Debus J, Bentzen SM, Daartz J, et al. Radiation oncology in the era of precision medicine. Nat Rev Cancer 2016;16:234-49.

[4] Newhauser WD, Zhang R. The physics of proton therapy. Phys Med Biol 2015;60:R155-209.

[5] Lomax AJ. Intensity modulated proton therapy and its sensitivity to treatment uncertainties 2: the potential effects of inter-fraction and inter-field motions. Phys Med Biol 2008;53:1043-56.

[6] Bert C, Durante M. Motion in radiotherapy: particle therapy. Phys Med Biol 2011;56:R113-44.

[7] Jaffray DA. Image-guided radiotherapy: from current concept to future perspectives. Nat Rev Clin Oncol 2012;9:688-99.

[8] Stuetzer K, Paessler T, Valentini C, Exner F, Thiele J, Hoelscher T, et al. SU-F-J-203: Retrospective Assessment of Delivered Proton Dose in Prostate Cancer Patients Based On Daily In-Room CT Imaging. Med Phys 2016;43:3455.

[9] Rit S, Clackdoyle R, Keuschnigg P, Steininger P. Filtered-backprojection reconstruction for a cone-beam computed tomography scanner with independent source and detector rotations. Med Phys 2016;43:2344.

[10] Shi W, Li JG, Zlotecki RA, Yeung A, Newlin H, Palta J, et al. Evaluation of kV cone-beam ct performance for prostate IGRT: a comparison of automatic grey-value alignment to implanted fiducial-marker alignment. Am J Clin Oncol 2011;34:16-21.

[11] Paluska P, Hanus J, Sefrova J, Rouskova L, Grepl J, Jansa J, et al. Utilization of cone-beam CT for offline evaluation of target volume coverage during prostate image-guided radiotherapy based on bony anatomy alignment. Rep Pract Oncol Radiother 2012;17:134-40.

[12] Guckenberger M, Meyer J, Wilbert J, Baier K, Sauer O, Flentje M. Precision of image-guided radiotherapy (IGRT) in six degrees of freedom and limitations in clinical practice. Strahlenther Onkol 2007;183:307-13.

[13] Trofimov A, Nguyen PL, Coen JJ, Doppke KP, Schneider RJ, Adams JA, et al. Radiotherapy treatment of early-stage prostate cancer with IMRT and protons: a treatment planning comparison. Int J Radiat Oncol Biol Phys 2007;69:444-53.

[14] Mendenhall NP, Malyapa RS, Su Z, Yeung D, Mendenhall WM, Li Z. Proton therapy for head and neck cancer: rationale, potential indications, practical considerations, and current clinical evidence. Acta Oncol 2011;50:763-71.

[15] Simone CB, 2nd, Ly D, Dan TD, Ondos J, Ning H, Belard A, et al. Comparison of intensity-modulated radiotherapy, adaptive radiotherapy, proton radiotherapy, and adaptive proton

radiotherapy for treatment of locally advanced head and neck cancer. Radiother Oncol 2011;101:376-82.

[16] Barker JL, Jr., Garden AS, Ang KK, O'Daniel JC, Wang H, Court LE, et al. Quantification of volumetric and geometric changes occurring during fractionated radiotherapy for head-and-neck cancer using an integrated CT/linear accelerator system. Int J Radiat Oncol Biol Phys 2004;59:960-70.

[17] Muller BS, Duma MN, Kampfer S, Nill S, Oelfke U, Geinitz H, et al. Impact of interfractional changes in head and neck cancer patients on the delivered dose in intensity modulated radiotherapy with protons and photons. Phys Med 2015;31:266-72.

[18] Stützer K, Jakobi A, Bandurska-Luque A, Barczyk S, Arnsmeyer C, Lock S, et al. Potential proton and photon dose degradation in advanced head and neck cancer patients by intratherapy changes. J Appl Clin Med Phys 2017;18:104-13.

[19] Beltran C, Herman MG, Davis BJ. Planning target margin calculations for prostate radiotherapy based on intrafraction and interfraction motion using four localization methods. Int J Radiat Oncol Biol Phys 2008;70:289-95.

[20] Padhani AR, Khoo VS, Suckling J, Husband JE, Leach MO, Dearnaley DP. Evaluating the effect of rectal distension and rectal movement on prostate gland position using cine MRI. Int J Radiat Oncol Biol Phys 1999;44:525-33.

[21] Bylund KC, Bayouth JE, Smith MC, Hass AC, Bhatia SK, Buatti JM. Analysis of interfraction prostate motion using megavoltage cone beam computed tomography. Int J Radiat Oncol Biol Phys 2008;72:949-56.

[22] Thornqvist S, Muren LP, Bentzen L, Hysing LB, Hoyer M, Grau C, et al. Degradation of target coverage due to inter-fraction motion during intensity-modulated proton therapy of prostate and elective targets. Acta Oncol 2013;52:521-7.

[23] Tang S, Deville C, Tochner Z, Wang KK, McDonough J, Vapiwala N, et al. Impact of intrafraction and residual interfraction effect on prostate proton pencil beam scanning. Int J Radiat Oncol Biol Phys 2014;90:1186-94.

[24] Thieke C, Kufer KH, Monz M, Scherrer A, Alonso F, Oelfke U, et al. A new concept for interactive radiotherapy planning with multicriteria optimization: first clinical evaluation. Radiother Oncol 2007;85:292-8.

[25] Cheung JP, Park PC, Court LE, Ronald Zhu X, Kudchadker RJ, Frank SJ, et al. A novel dose-based positioning method for CT image-guided proton therapy. Med Phys 2013;40:051714.

[26] Haehnle J, Suss P, Landry G, Teichert K, Hille L, Hofmaier J, et al. A novel method for interactive multi-objective dose-guided patient positioning. Phys Med Biol 2017;62:165-85.

[27] Hofmaier J, Haehnle J, Kurz C, Landry G, Maihoefer C, Schuttrumpf L, et al. Multi-criterial patient positioning based on dose recalculation on scatter-corrected CBCT images. Radiother Oncol 2017;125:464-9.

[28] Wohlfahrt P, Mohler C, Hietschold V, Menkel S, Greilich S, Krause M, et al. Clinical Implementation of Dual-energy CT for Proton Treatment Planning on Pseudo-monoenergetic CT scans. Int J Radiat Oncol Biol Phys 2017;97:427-34.

[29] Marks LB, Yorke ED, Jackson A, Ten Haken RK, Constine LS, Eisbruch A, et al. Use of normal tissue complication probability models in the clinic. Int J Radiat Oncol Biol Phys 2010;76:S10-9.

[30] Stockle M, Bussar-Maatz R. [Localised prostate cancer: the PREFERE trial]. Z Evid Fortbild Qual Gesundhwes 2012;106:333-5; discussion 5.

[31] Monz M, Kufer KH, Bortfeld TR, Thieke C. Pareto navigation: algorithmic foundation of interactive multi-criteria IMRT planning. Phys Med Biol 2008;53:985-98.

[32] Miettinnen K. Nonlinear multiobjective optimization: Kluwer Academic Publishers; 1999.

[33] Landry G, Nijhuis R, Dedes G, Handrack J, Thieke C, Janssens G, et al. Investigating CT to CBCT image registration for head and neck proton therapy as a tool for daily dose recalculation. Med Phys 2015;42:1354-66.

[34] Park YK, Sharp GC, Phillips J, Winey BA. Proton dose calculation on scatter-corrected CBCT image: Feasibility study for adaptive proton therapy. Med Phys 2015;42:4449-59.

[35] Kurz C, Kamp F, Park YK, Zollner C, Rit S, Hansen D, et al. Investigating deformable image registration and scatter correction for CBCT-based dose calculation in adaptive IMPT. Med Phys 2016;43:5635.

[36] Veiga C, McClelland J, Moinuddin S, Lourenco A, Ricketts K, Annkah J, et al. Toward adaptive radiotherapy for head and neck patients: Feasibility study on using CT-to-CBCT deformable registration for "dose of the day" calculations. Med Phys 2014;41:031703-1-12.

[37] Gu X, Pan H, Liang Y, Castillo R, Yang D, Choi D, et al. Implementation and evaluation of various demons deformable image registration algorithms on a GPU. Phys Med Biol 2010;55:207-19.

[38] Thor M, Petersen JB, Bentzen L, Hoyer M, Muren LP. Deformable image registration for contour propagation from CT to cone-beam CT scans in radiotherapy of prostate cancer. Acta Oncol 2011;50:918-25.

[39] Thornqvist S, Petersen JB, Hoyer M, Bentzen LN, Muren LP. Propagation of target and organ at risk contours in radiotherapy of prostate cancer using deformable image registration. Acta Oncol 2010;49:1023-32.

[40] Ma L, Guo R, Zhang G, Tade F, Schuster D, Nieh P, et al. Automatic segmentation of the prostate on CT images using deep learning and multi-atlas fusion. Proceedings Volume 10133, Medical Imaging 2017: Image Processing 2017.

[41] Kazemifar S, Balagopal A, Nguyen D, McGuire S, Hannan H, Jiang S, et al. Segmentation of the prostate and organs at risk in male pelvic CT images using deep learning. arXiv:180209587 2018.

Figures

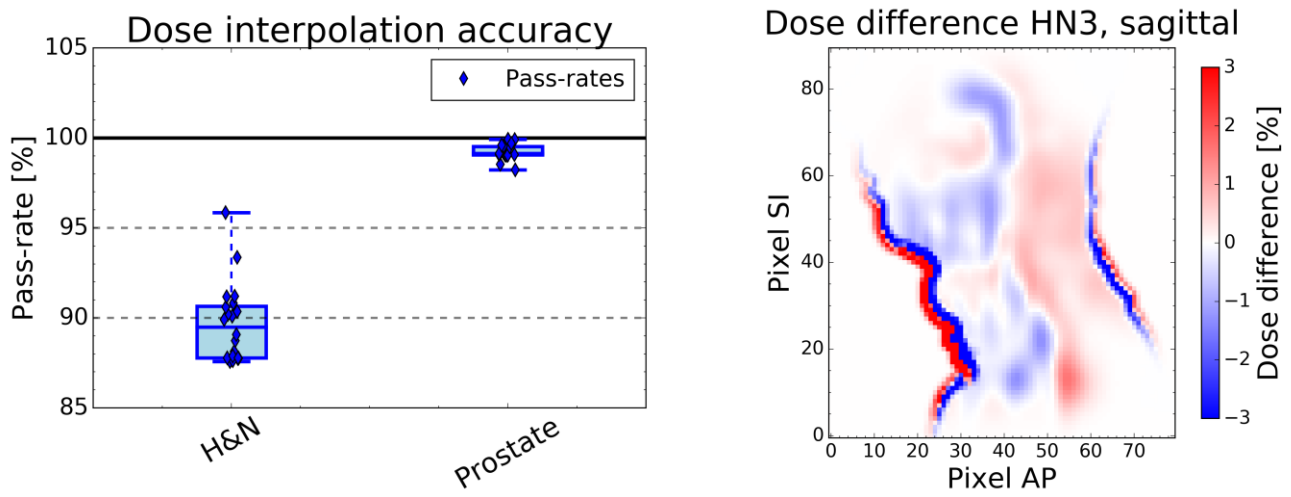

Figure 1. Boxplot of the pass-rates for the 2% dose-difference criterion at 20 random shifts for an exemplary H&N (HN3) and prostate (PRO1) patient (left). A sagittal slice of patient HN3 at the automatically determined optimal shift according to the clinical goals shows that deviations between interpolated and exact dose are confined at the outer contour of the patient (right).

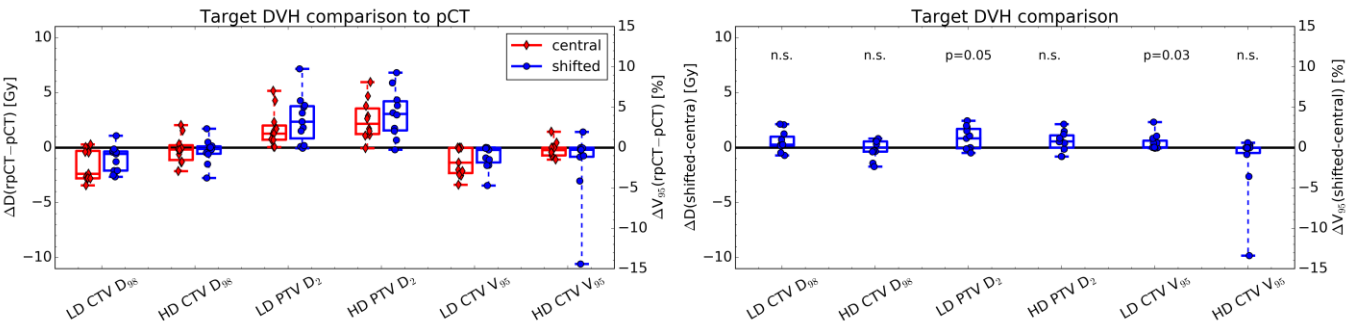

Figure 2. Boxplot of changes in target DVH parameters for the H&N IMPT cohort. On the left, changes with respect to the initial planning scenario (pCT) are shown for the anatomy-based alignment (central, red) and the determined optimal dose-guided shift (shifted, blue), both evaluated on the rpCT. On the right, DVH parameters for central and shifted dose on the rpCT are directly compared. Statistically significant differences are indicated by the corresponding p-value. Non-significant differences are indicated by 'n.s.'. All values are given for the whole course of fractionated treatment.

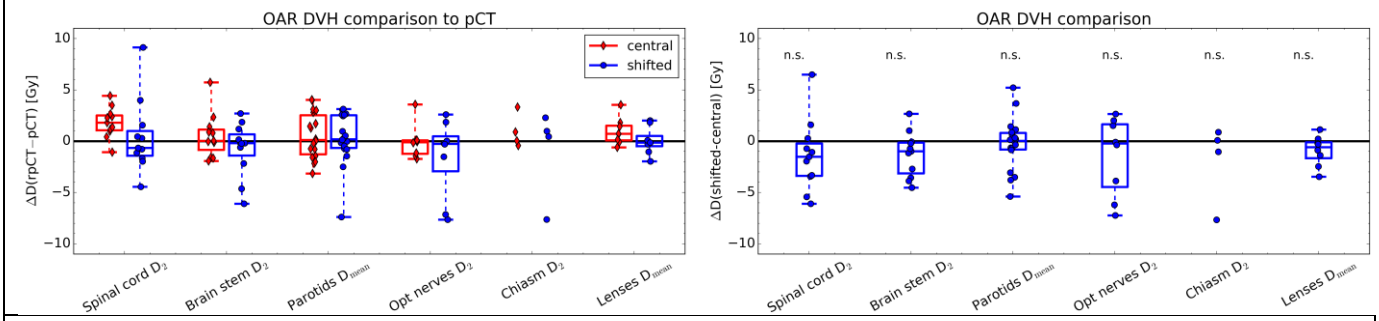

Figure 3. Boxplot of changes in OAR DVH parameters for the H&N IMPT cohort. On the left, changes with respect to the initial planning scenario (pCT) are shown for the anatomy-based alignment (central, red) and the dose-guided shift (shifted, blue) on the rpCT. On the right, DVH parameters for central and shifted dose on the rpCT are directly compared. Non-significant differences are indicated by 'n.s.'. All values are given for the whole course of fractionated treatment.

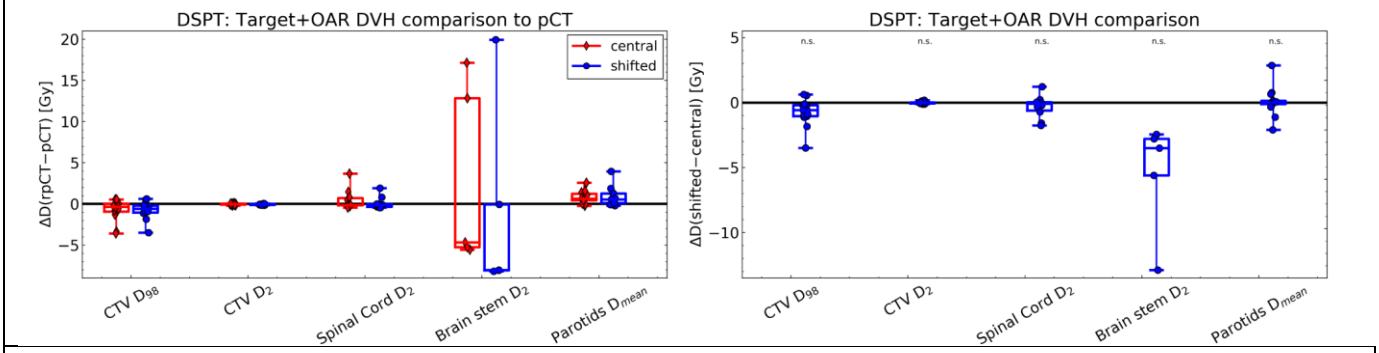

Figure 4. Boxplot of changes in Target and OAR DVH parameters for the H&N DSPT cohort. On the left, changes with respect to the initial planning scenario (pCT) are shown for the anatomy-based alignment (central, red) and the dose-guided shift (shifted, blue) on the rpCT. On the right, DVH parameters for central and shifted dose on the rpCT are directly compared. Non-significant differences are indicated by 'n.s.'. All values are given for the whole course of fractionated treatment.

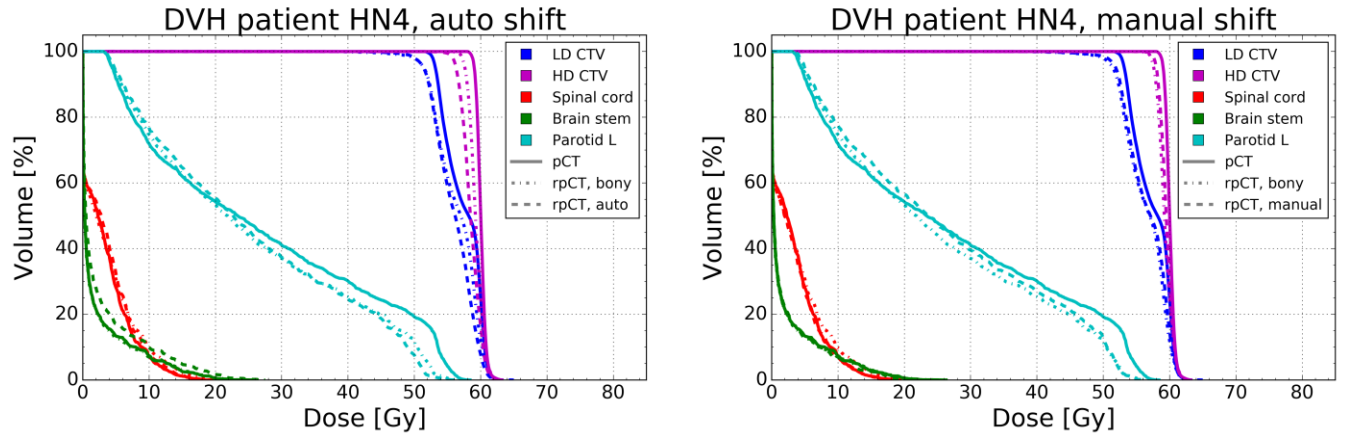

Figure 5. DVH curve comparison for patient HN4. Original planning scenario on pCT (solid) and bony-anatomy-based alignment of the rpCT (dotted) are compared to the dose-guided shift (dashed) of the rpCT. The left panel shows the DVH curves for the automatically determined dose-guided shift according to the defined clinical goals, the right panel for the manually determined dose-guided shift.

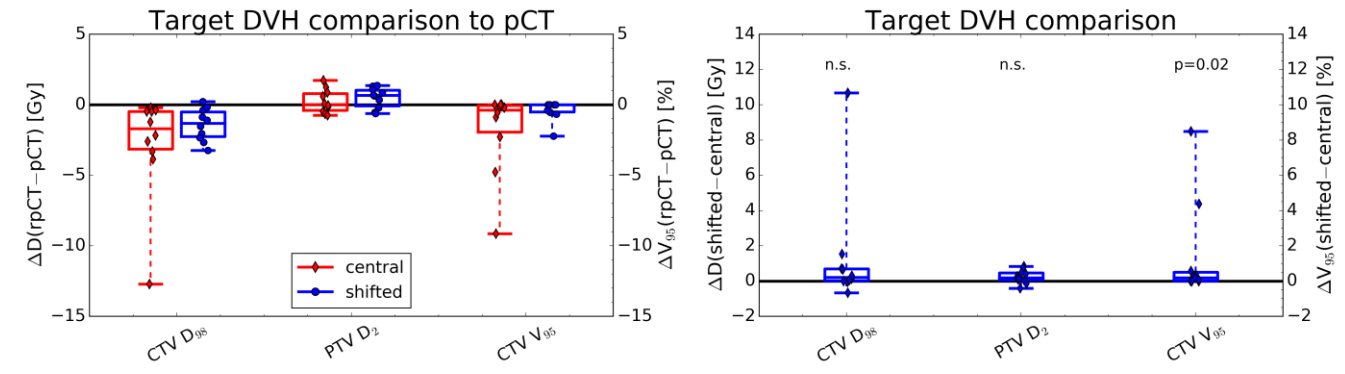

Figure 6. Boxplot of changes in target DVH parameters for the prostate IMPT cohort. On the left, changes with respect to the initial planning scenario (pCT) are shown for anatomy-based alignment (central, red) and optimal dose-guided shift (shifted, blue) on the rpCT. On the right, DVH parameters for central and shifted dose on the rpCT are compared. Statistically significant differences are indicated by the corresponding p-value. Non-significant differences are indicated by 'n.s.'. All values are given for the whole course of fractionated treatment.

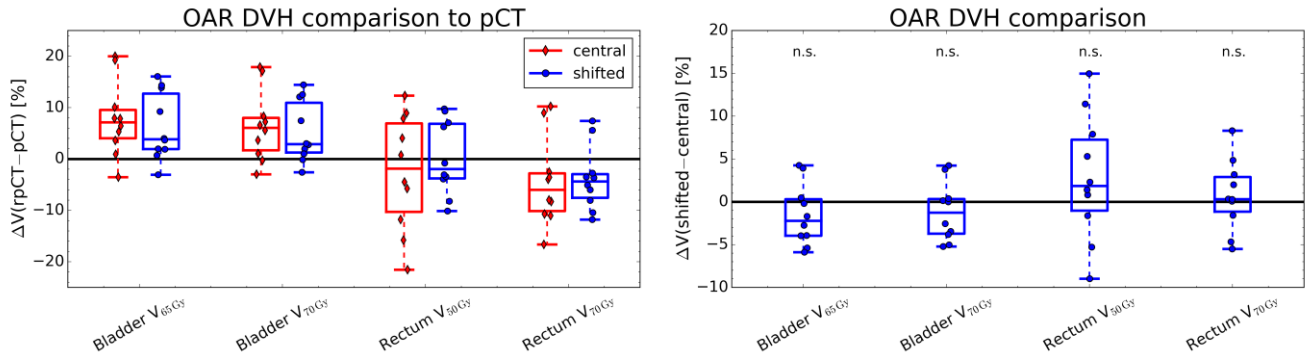

Figure 7. Boxplot of changes in OAR DVH parameters for the prostate IMPT cohort. On the left, changes with respect to the initial planning scenario (pCT) are shown for the anatomy-based alignment (central, red) and the determined optimal shift (shifted, blue) on the rpCT. On the right, DVH parameters for central and shifted dose on the rpCT are directly compared. Non-significant differences are indicated by 'n.s.'.

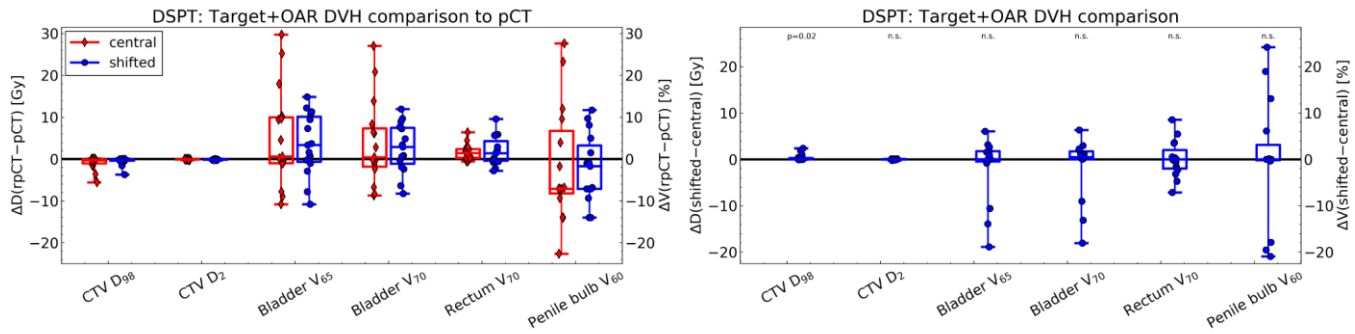

Figure 8. Boxplot of changes in Target and OAR DVH parameters for the prostate DSPT cohort. On the left, changes with respect to the initial planning scenario (pCT) are shown for the anatomy-based alignment (central, red) and the determined optimal shift (shifted, blue) on the rpCT. On the right, DVH parameters for central and shifted dose on the rpCT are directly compared. Non-significant differences are indicated by 'n.s.'. All values are given for the whole course of fractionated treatment.

Tables

Patients	Structure	Clinical goal DGP	Importance class
HN1-14	High and low dose CTV	$D_{98\%} > D_{98\%,pCT}$	1
	High and low dose PTV	$D_{2\%} < D_{2\%,pCT}$	1
	Brain stem	$D_{2\%} < 54$ Gy	0
		$D_{2\%} < D_{2\%,pCT}$	1
	Spinal Cord	$D_{2\%} < 45$ Gy	0
		$D_{2\%} < D_{2\%,pCT}$	1
	Parotid glands	$D_{mean} < D_{mean,pCT}$	1
HN8-11	Optical nerves	$D_{2\%} < D_{2\%,pCT}$	1
	Optical chiasm	$D_{2\%} < D_{2\%,pCT}$	1
	Eye Lenses	$D_{mean} < D_{mean,pCT}$	1
PRO1-8	CTV	$D_{98\%} > D_{98\%,pCT}$	1
	PTV	$D_{2\%} < D_{2\%,pCT}$	1
	Rectum	$V_{70Gy} < V_{70Gy,pCT}$	1
	Bladder	$V_{65Gy} < V_{65Gy,pCT}$	1
		$V_{70Gy} < V_{70Gy,pCT}$	1
PRO6-8	Femoral heads	$V_{50Gy} < V_{50Gy,pCT}$	1
	Penile bulb	$V_{60Gy} < V_{60Gy,pCT}$	1

Table 1. Overview of the clinical goals used for dose-guided positioning (DGP) in this study. The subscript *pCT* indicates that for the corresponding DVH parameter the deviation with respect to the planning scenario was evaluated.

Patient	rpCT	Shift in mm			Pass-rate in %
		LR	AP	SI	
HN1	1	0.0	3.7	0.0	95.14
HN2	1	0.0	-0.2	-2.9	99.69
HN3	1	0.4	-3.8	0.7	88.32
HN4	1	0.0	0.0	3.0	100.00
HN5	1	0.0	0.0	-6.0	100.00
HN6	1	0.0	-0.1	-3.9	94.93
HN7	1	-1.2	-1.8	0.0	90.90
HN8	1	-1.1	0.4	1.0	94.11
HN9	1	0.0	-0.6	-3.0	95.17
HN10	1	0.0	0.0	-3.0	100.00
HN11	1	0.0	0.0	-6.0	100.00
HN12	1	0.0	-6.0	0.0	100.00
	2	0.0	-6.0	0.0	100.00
	3	0.0	-6.0	0.0	100.00
	4	0.0	0.0	-4.2	96.52
	5	0.0	0.0	6.0	100.00
HN13	1	0.0	0.0	0.0	100.00
	2	0.0	-2.3	1.8	75.99
	3	0.0	-0.9	4.1	79.84
	4	0.0	-5.1	-0.5	89.13
	5	0.0	-2.8	1.6	79.21
HN14	1	3.0	0.0	0.0	100.00
	2	3.0	0.0	0.0	100.00
	3	-3.0	0.0	0.0	100.00
	4	0.0	-3.0	0.0	100.00

Table 2. Determined shifts (with respect to the anatomy-based alignment) according to the pre-defined clinical goals for all H&N patients. The pass-rates for the comparison of exact and interpolated dose using a 2% dose-difference criterion at the respective shifts are also given. The horizontal line separates the IMPT and DSPT cohorts.

Patient	rpCT	Shift in mm			Pass-rate in %
		LR	AP	SI	
PRO1	1	0.0	6.0	0.0	100.00
	2	0.0	0.0	-3.0	100.00
PRO2	1	0.0	3.0	0.0	100.00
	2	0.0	6.0	0.0	100.00
PRO3	1	0.0	0.0	-3.0	100.00
	2	0.0	3.0	0.0	100.00
PRO4	1	0.0	-3.0	0.0	100.00
	2	0.0	0.0	-3.0	100.00
PRO5	1	0.0	-3.0	0.0	100.00
	2	-4.2	-0.9	0.0	97.90
PRO6	1	0.0	-3.0	0.0	100.00
	2	3.0	0.0	0.0	100.00
	3	6.0	0.0	0.0	100.00
	4	0.0	0.0	3.0	100.00
	5	0.0	-3.0	0.0	100.00
PRO7	1	0.0	-2.6	-1.7	98.81
	2	-6.0	0.0	0.0	100.00
	3	4.8	-0.1	-0.5	95.23
	4	-0.2	1.9	-1.0	99.06
	5	-6.0	0.0	0.0	100.00
PRO8	1	0.0	0.0	3.0	100.00
	2	0.0	0.0	6.0	100.00
	3	0.0	6.0	0.0	100.00
	4	-4.1	-0.5	0.5	94.70
	5	0.0	3.2	0.8	99.53

Table 3. Determined shifts (with respect to the anatomy-based alignment) according to the pre-defined clinical goals for all prostate patients and pass-rates for comparison of exact and interpolated dose using a 2% dose-difference criterion at the respective shift. The horizontal line separates the IMPT and DSPT cohorts.